Available online at www.rajournals.in

RA JOURNAL OF APPLIED RESEARCH
ISSN: 2394-6709
DOI:10.47191/rajar/v10i05.01
Volume: 10 Issue: 05 May-2024

International Open Access

Impact Factor- 8.174

Page no.- 95-102

High Temperature Solid Oxide Electrolyte Fuel Cell Formulation: Non-Steady State Utilization of Fuel and Oxidant

S.S. Sandhu[1,*], K.R. Hinkle[2]

[1,2]Department of Chemical and Materials Engineering, University of Dayton, 300 College Park, Dayton, OH 45469-0246, USA

ARTICLE INFO

Published Online:
02 May 2024

Corresponding Author:
S.S. Sandhu

ABSTRACT

The formulation presented in this paper was developed with the objective of its application to investigate the transient behavior of a high temperature solid oxide fuel cell (SOFC); especially with respect to the non-steady state consumption of fuel and oxidant reactants. Specifically, the chemical species transient amounts, their mole fractions, and total pressures in the cell anode-side fuel- (hydrogen) and cathode-side oxidant- (oxygen of the air) chambers can be predicted under the isothermal condition at a fixed cell-current level. The developed formulation is also capable of predicting the transient mole fraction profiles of fuel (hydrogen) and oxidant (oxygen) in the cell porous anode and cathode, respectively; thus, providing insight into the reactant species' effective transport and their utilization, via electrochemical reactions, in the cell porous electrodes. The presented formulation can be adapted for any fuel and oxidant combinations in any high temperature SOFC.

1. INTRODUCTION

The work presented here is a continuation and extension of our previous findings [1] which focused on formulating thermodynamic descriptions of SOFCs operating under steady-state conditions. Figure 1 shows the sketch of a generic electrolyte fuel cell. It is composed of three major components: Anode, A; electrolyte separator, Electro; and cathode, C.

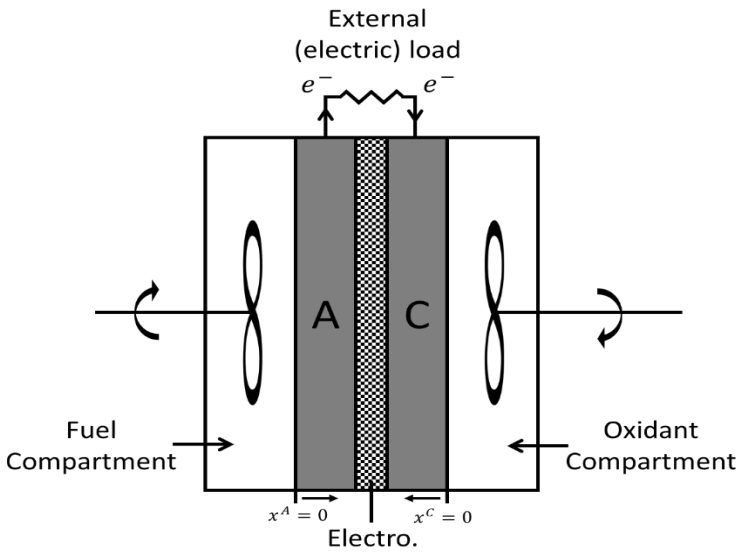

Figure 1. Representation of a model high temperature solid oxide electrolyte fuel cell (the sketch not- to- a scale).

The SOFC cell shown in Figure 1 is explained as follows: The cell anode, A: A cermet of metallic nickel (NiO(s) in the absence of a reducing environment) and yttria, $Y_2O_3(s)$, stabilized zirconia, $ZrO_2(s)$, with a porosity (e.g. 16 – 30%) to facilitate the transfer of reactant and product gaseous species. The cell electrolyte, (denoted Electro): A thin film of

yttria-stabilized zirconia; yttria doping is required to stabilize the cubic crystal structure of zirconia as well as for the creation of the oxygen vacancy defects required for the enhancement of ionic transport of oxide ions (O^{2-}). A typical composition of the solid oxide electrolyte is: yttria (16.9%) and zirconia (83.1%) by weight. The cell cathode, C: Porous strontium-doped lanthanum manganite, $La_{1-x}Sr_xMnO_3$ $(0.10 < x < 0.18)$; a *p*-type semiconductor. The strontium doping bestows the p-type electronic conductivity by the creation of electron holes. Other materials; particularly *p*-type conducting perovskite structures display mixed electronic and ionic conductivity. The perovskites; lanthanum strontium ferrite, lanthanum strontium cobaltite as well as *n*-type semiconductors are better electrocatalysts than the state-of-the-art lanthanum strontium manganite [2]. A porous structure (e.g. porosity of 20 – 40%) is required for rapid mass transport of reactant/ product species.

For the model formulation presented in this work, the fuel and oxidant mixtures in their storage chambers are stirred to prevent the formation of concentration boundary layers at the cell porous anode and cathode planar surfaces located at the $x^A = 0$ and $x^C = 0$ planes; thus resulting in the reduction of the resistance to mass transfer of the reactive species to the respective surfaces of the cell electrode. This would result in the lowering of the cell voltage loss associated with the build-up of such concentration boundary layers (films) under the non-stirred fuel and oxidant mixtures.

2. The SOFC Formulation: Cell operational conditions of isothermal and non-steady state utilization of reactant species

2.1 Determination of Compositions and Pressures within the Fuel and Oxidant Compartments

Under a constant current cell operation, the cell anode-side reactant (hydrogen) and cathode-side reactant (oxygen) are required to be consumed at constant rates to maintain the cell current at a desired constant level. Under non-steady state cell operation, the reactant concentrations in the storage chambers decrease with an increase in operational cell period. Depending on the magnitude of the cell current, there would be build-up of reactant species concentration boundary-layers around the three-phase contact points where the reactant species are consumed and the product species are generated via the electrochemical reactions in the cell porous anode and cathode electrodes. Consequently, this would result in an increase in the resistance to mass transfer of reactant and product species, respectively, to and away from the electro-active three-phase contact points. However, the probability of build-up of concentration boundary layers at the cell electrode planar surfaces at $x^A = 0$ and $x^C = 0$ locations would be negligible; especially under the vigorously stirred conditions in the reactant and product species storage chambers. The overall cell voltage loss would occur due to the voltage-loss associated with the species mass transfer in the relatively thick electrodes; especially, at high delivery of cell currents. At a controlled constant current delivery, the cell voltage loss associated with the transport of oxide ions (O^{2-}) through the electrolyte separator between the electrodes would remain invariant under the cell isothermal operational condition. Therefore, with an increase in the cell electric-power delivery time; the increase in the cell voltage loss is due to the coupled effect of the increase in species mass transfer-related resistance in porous electrodes and the probable variations in the interfacial current density per unit electro-active area and in the interfacial areas per unit bed volume in both the cell electrodes.

The formulation presented in this work is for hydrogen (fuel) and air (oxidant) for the model cell sketched in Figure 1. The notation for the various components of the sketched SOFC is as follows: v^A and v^C represent the volume of the cell anode- and cathode-side fuel and oxidant compartments; A^A and A^C represent the planar geometric surface areas of the cell anode and cathode at the $x^A = 0$ and $x^C = 0$ locations; ℓ^A, ℓ^E, and ℓ^C denote the thickness of the cell anode, electrolyte separator, and cathode, respectively. The cell anode-side fuel compartment is assumed to initially contain $n^A_{H_2(g),init}$ moles of hydrogen gas in the mixture of hydrogen and water vapor. The initial hydrogen composition of the mixture is $y_{H_2(g),init}$; therefore, the initial amount of water vapor in the fuel compartment is:

$$n^A_{H_2O(v),init} = \left(\frac{y^A_{H_2O(v),init}}{y^A_{H_2(g),init}}\right) n^A_{H_2(g),init} \tag{1}$$

Where the mole fraction of water vapor in the initial hydrogen-water vapor mixture is $y^A_{H_2O(v),init} = \left(1 - y^A_{H_2(g),init}\right)$.

The total initial amount of hydrogen gas (fuel)-water vapor mixture is,

$$n^A_{tot,init} = \frac{n^A_{H_2(g),init}}{y^A_{H_2(g),init}} \tag{2}$$

The overall cell reaction is:

$$H_2(g) + \frac{1}{2}O_2(g) \rightarrow H_2O(v) \tag{3}$$

For the complete utilization of hydrogen gas, the amount of oxygen required by stoichiometry is,

$$n^A_{O_2(g),stoich} = \frac{n^A_{H_2(g),init}}{2} \tag{4}$$

At the level of 5 mole % of excess oxygen, the required initial amount of oxygen in the cell cathode-side oxidant storage chamber is,

$$n^C_{O_2(g),init} = 1.05 n^A_{O_2(g),stoich} = \left(\frac{1.05}{2}\right) n^A_{H_2(g),init} = 0.525 n^A_{H_2(g),init} \quad (5)$$

Also, the amount of excess oxygen present is:

$$n^C_{O_2(g),ex} = (0.525 - 0.5) n^A_{H_2(g),init} = 0.025 n^A_{H_2(g),init} \quad (5a)$$

The initial amount of dry air in the cell cathode-side oxidant chamber is,

$$n^C_{dry\ air,init} = \frac{n^C_{O_2(g),init}}{y^C_{O_2(g),air}} = \frac{0.525}{0.21} n^A_{H_2(g),init} = 2.5 n^A_{H_2(g),init} \quad (6)$$

The amount of nitrogen in the initial gas mixture in the oxidant chamber is,

$$n^C_{N_2(g),init} = 0.79 n^C_{dry\ air,init} = 0.79\left(2.5 n^A_{H_2(g),init}\right) = 1.975 n^A_{H_2(g),init} \quad (7)$$

If the cell cathode-side oxidant compartment initially contains air -water vapor mixture with water vapor at the mole fraction level of $y^C_{H_2O(v),init}$; then the total initial amount of air plus water vapor is given by:

$$n^C_{tot,init} = \frac{n^C_{dry\ air,init}}{1 - y^C_{H_2O(v),init}} = \frac{2.5 n^A_{H_2(g),init}}{1 - y^C_{H_2O(v),init}} \quad (8)$$

Also, the initial amount of water vapor in the oxidant chamber is given by

$$n^C_{H_2O(v),init} = 2.5 \left(\frac{y^C_{H_2O(v),init}}{1 - y^C_{H_2O(v),init}}\right) n^A_{H_2(g),init} \quad (9)$$

The electrochemical reactions occurring in the cell anode and cathode during the period of the electric power production and delivery to an external electric load circuit are given as follows:

In the cell porous anode:

$$H_2(g) \rightarrow 2H^+ + 2e^-$$
$$2H^+ + O^{2-} \rightarrow H_2O(v) \quad (10)$$

With the overall anode reaction being:

$$H_2(g) + O^{2-} \rightarrow H_2O(v) + 2e^- \quad (11)$$

In the cell porous cathode:

$$\frac{1}{2} O_2(g) + 2e^- \rightarrow O^{2-} \quad (12)$$

If the model SOFC (Figure 1) is to be operated at a constant current level of I amperes; the hydrogen and oxide-anion consumption rates, and the water vapor production rate are given as follows:

$$\dot{n}^A_{H_2(g)} = -\frac{I}{2F} \quad (13)$$

$$\dot{n}^A_{O^{2-}} = -\frac{I}{2F} \quad (14)$$

$$\dot{n}^A_{H_2O(v)} = +\frac{I}{2F} \quad (15)$$

Correspondingly, the oxygen consumption and oxide-anion production rates in the cell porous- cathode are given by:

$$\dot{n}^C_{O_2(g)} = -\frac{I}{4F} \quad (16)$$

$$\dot{n}^C_{O^{2-}} = +\frac{I}{2F} \quad (17)$$

Equations (14) and (17) show that the oxide-anion consumption and production rates are numerically equal. This implies that the oxide-anion transport rate through the cell electrolyte separator, (Electro. in Figure 1), from the cell cathode to anode is required to be equal to $I/2F$ $(mol \cdot s^{-1})$ at the constant current level of I amperes. The consumed and produced amounts of the various species during the cell operational time of (t seconds) are given as follows:

$$\Delta n^A_{H_2(g)} = -\frac{I}{2F} t \quad (18)$$

$$\Delta n^A_{H_2O(v)} = +\frac{I}{2F} t \quad (19)$$

$$\Delta n^C_{O_2(g)} = -\frac{I}{4F} t \quad (20)$$

$$\Delta n^C_{O^{2-}} = +\frac{I}{2F} t \quad (21)$$

It is here mentioned that the only overall reactions occurring in the model cell system (Figure 1) are the ones represented by Equations (3), (11) and (12). Therefore, the amounts of the various chemical species in the cell anode-side fuel and cathode-side oxidant compartments can be written as functions of time, t, as follows:

$$n^A_{H_2(g)}(t) = n^A_{H_2(g),init}\left(1 - \frac{I}{2F n^A_{H_2(g),init}} t\right) \quad (22)$$

$$n^A_{H_2O(v)}(t) = n^A_{H_2(g),init}\left(\frac{1-y^A_{H_2(g),init}}{y^A_{H_2(g),init}} + \frac{I}{2Fn^A_{H_2(g),init}}t\right) \quad (23)$$

$$n^C_{O_2(g)}(t) = n^A_{H_2(g),init}\left(0.525 - \frac{I}{4Fn^A_{H_2(g),init}}t\right) \quad (24)$$

$$n^C_{N_2(g)}(t) = n^C_{N_2(g),init} = 1.975n^A_{H_2(g),init} \quad (25)$$

$$n^C_{H_2O(v)}(t) = n^C_{H_2O(v),init} = 2.5\left(\frac{y^C_{H_2O(v),init}}{1-y^C_{H_2O(v),init}}\right)n^A_{H_2(g),init} \quad (26)$$

The total amount of charge passed through the external electrical load circuit in time (t seconds) is given by

$$Q_{charge}(t) = I \cdot t \quad (27)$$

At the end of the cell operational time of (t seconds), the total species mixture moles in the cell anode-side and cathode-side species-storage compartments are given as follows:

$$n^A_{tot}(t) = n^A_{H_2(g)}(t) + n^A_{H_2O(v)}(t) = n^A_{tot,init} = \frac{n^A_{H_2(g),init}}{y^A_{H_2(g),init}} \quad (28)$$

$$n^C_{tot}(t) = n^C_{O_2(g)}(t) + n^C_{N_2(g)}(t) + n^C_{H_2O(v)}(t) = 2.5\frac{n^A_{H_2(g),init}}{1-y^C_{H_2O(v),init}} - \frac{I}{4F}t \quad (29)$$

Equations 28 and 29 can then be used to write the chemical species mole fractions in the anode-side and cathode-side compartments as functions of time:

$$y^A_{H_2(g)}(t) = \frac{n^A_{H_2(g)}}{n^A_{tot}} = y^A_{H_2(g),init}\left(1 - \frac{I}{2Fn^A_{H_2(g),init}}t\right) \quad (30)$$

$$y^A_{H_2O(v)}(t) = \frac{n^A_{H_2O(v)}}{n^A_{tot}} = y^A_{H_2(g),init}\left(\frac{1-y^A_{H_2(g),init}}{y^A_{H_2(g),init}} + \frac{I}{2Fn^A_{H_2(g),init}}t\right) \quad (31)$$

$$y^C_{O_2(g)}(t) = \frac{n^C_{O_2(g)}}{n^C_{tot}} = \frac{\left(0.525 - \frac{I}{4Fn^A_{H_2(g),init}}t\right)}{\left(\frac{2.5}{1-y^C_{H_2O(v),init}} - \frac{I}{4Fn^A_{H_2(g),init}}t\right)} \quad (32)$$

$$y^C_{N_2(g)}(t) = \frac{n^C_{N_2(g)}}{n^C_{tot}} = \frac{1.975}{\left(\frac{2.5}{1-y^C_{H_2O(v),init}} - \frac{I}{4Fn^A_{H_2(g),init}}t\right)} \quad (33)$$

$$y^C_{H_2O(v)}(t) = \frac{n^C_{H_2O(v)}}{n^C_{tot}} = \frac{2.5\left(\frac{y^C_{H_2O(v),init}}{1-y^C_{H_2O(v),init}}\right)}{\left(\frac{2.5}{1-y^C_{H_2O(v),init}} - \frac{I}{4Fn^A_{H_2(g),init}}t\right)} \quad (34)$$

Total pressures in the cell anode-side and cathode-side compartments at the initial state conditions are given as the following functions of time:

$$p^A_{tot}(t) = p^A_{tot,init} = \frac{n^A_{H_2(g),init}}{y^A_{H_2(g),init}}\left(\frac{RT}{v^A}\right) \quad (35)$$

$$p^C_{tot,init} = n^C_{tot,init}\left(\frac{RT}{v^C}\right) = 2.5\frac{n^A_{H_2(g),init}}{1-y^C_{H_2O(v),init}}\left(\frac{RT}{v^C}\right) \quad (36)$$

$$p^C_{tot}(t) = n^C_{tot}\left(\frac{RT}{v^C}\right) = \left(2.5\frac{n^A_{H_2(g),init}}{1-y^C_{H_2O(v),init}} - \frac{I}{4F}t\right)\left(\frac{RT}{v^C}\right) \quad (37)$$

The time for complete utilization of the cell fuel, t_f, at a constant current level of I amperes, is given by

$$t_f = \frac{2F}{I}n^A_{H_2(g),init} \quad (38)$$

At the complete utilization of cell fuel, the SOFC would stop providing electric power to an external electrical load circuit. At this system state, the chemical species mole fractions in the fuel and oxidant compartments are given as follows:

$$y^A_{H_2(g)}(t_f) = 0 \quad (39)$$

$$y^A_{H_2O(v)}(t_f) = 1 \quad (40)$$

$$y^C_{O_2(g)}(t_f) = \frac{0.025\left(1-y^C_{H_2O(v),init}\right)}{2-0.5y^C_{H_2O(v),init}} \quad (41)$$

$$y^C_{N_2(g)}(t_f) = \frac{1.975\left(1-y^C_{H_2O(v),init}\right)}{2-0.5y^C_{H_2O(v),init}} \quad (42)$$

$$y^C_{H_2O(v)}(t_f) = \frac{2.5y^C_{H_2O(v),init}}{2-0.5y^C_{H_2O(v),init}} \quad (43)$$

At the same time, t_f, following the consumption of fuel, the total pressures in the cell anode-side and cathode-side compartments are given as follows:

$$p^A_{tot}(t_f) = \frac{n^A_{H_2(g),init}}{y^A_{H_2(g),init}}\left(\frac{RT}{v^A}\right) \quad (44)$$

$$p_{tot}^{C}(t_f) = n_{tot}^{C}(t_f)\left(\frac{RT}{v^C}\right)$$
$$= \left(2.5\frac{n_{H_2(g),init}^{A}}{1-y_{H_2O(v),init}^{C}} - \frac{I}{4F}t_f\right)\left(\frac{RT}{v^C}\right) \quad (45)$$

2.2. Determination of Fuel Composition with the Cell Anode

Performing a mole balance for the reactant hydrogen fuel over a spatial element of thickness Δx^A located between the x^A and $x^A + \Delta x^A$ planes in the cell porous anode yields the following partial differential equation,

$$\frac{\partial \phi}{\partial \tau^A} = \frac{\partial^2 \phi}{\partial \zeta^2} - \lambda^A \phi \quad (46)$$

Here ϕ represents the dimensionless mol fraction of H_2 ($y_{H_2(g)}^{A}/y_{H_2(g),init}^{A}$) and is a function of both time and spatial dimension. ζ is the dimensionless spatial parameter (x^A/ℓ^A) and τ^A the dimensionless time defined as:

$$\tau^A = \frac{D_{H_2,eff}^{A}}{\varepsilon_{pore}^{A}(\ell^A)^2}\cdot t \quad (47)$$

Where $D_{H_2,eff}^{A}$ is the effective mass diffusivity of hydrogen in the cell porous anode and ε_{pore}^{A} is the pore volume fraction within the anode. The parameter λ^A in Equation 46 is a dimensionless quantity indicative of the electrochemical reaction rate and is represented as:

$$\lambda^A = \frac{2k^A S_{eff}^{A}\rho_{bulk}^{A}(\ell^A)^2}{D_{H_2,eff}^{A}}\sinh\left(\frac{F\bar{\eta}_s^A}{RT}\right) \quad (48)$$

Here k^A is the intrinsic reaction rate coefficient at the temperature of interest, S_{eff}^{A} is the effective interfacial area between the reactive gaseous mixture and the porous anode ρ_{bulk}^{A} is the bulk density of the composite solid in the cell anode, and $\bar{\eta}_s^A$ is the electrochemical reaction surface overpotential averaged over the thickness of the anode. The suitable set of the initial condition (IC) and boundary conditions (BC1 and BC2) to solve the PDE, Eq. (46), are given as follows:

$$IC: \quad \phi(\tau^A = 0) = 1 \quad for\ all\ \zeta \in [0,1] \quad (49)$$

$$BC1: \quad \phi(\zeta = 0) = 1 - \alpha^A\tau^A \quad for\ all\ \tau^A \in \left[0, \frac{1}{\alpha^A}\right] \quad (50)$$

$$BC2: \quad \left.\frac{d\phi}{d\zeta}\right|_{\zeta=1} = 0 \quad for\ all\ \tau^A \in \left[0, \frac{1}{\alpha^A}\right] \quad (51)$$

Here BC1 (Eq. 50) is a dimensionless form of Eq. 30, where α^A is a dimensionless quantity defined as:

$$\alpha^A = \frac{I\varepsilon_{pore}^{A}(\ell^A)^2}{2Fn_{H_2(g),init}^{A}D_{H_2,eff}^{A}} \quad (52)$$

This PDE has been solved analytically for the following two cases:

<u>*Case I*</u>

The porous cell anode is sufficiently thin (e.g. $\ell^A < 25\ \mu m$) that spatial variation due to diffusion within the anode can be neglected. Consequently, the PDE reduces to:

$$\frac{d\phi}{d\tau^A} = -\lambda^A\phi \quad (53)$$

Which has solution:

$$\phi(\tau^A) = e^{-\lambda^A\tau^A} \quad (54)$$

<u>*Case II*</u>

The porous cell anode is thick enough (e.g. $\ell^A = 1\ mm$) that spatial variations due to diffusion within the anode must be considered. Here the full PDE was solved analytically to yield $\phi(\tau^A, \zeta)$ as a function of both time and depth in the porous anode.

2.3. Determination of Oxidant Composition within Cell Cathode

Performing a mole balance for the reactant oxygen over a spatial element of thickness Δx^C located between the x^C and $x^C + \Delta x^C$ planes in the cell porous cathode yields the following partial differential equation,

$$\frac{\partial \psi}{\partial \tau^C} = \frac{\partial^2 \psi}{\partial \xi^2} - \left(\lambda^C - \frac{1}{\gamma^C - \tau^C}\right)\psi \quad (55)$$

Here ψ represents the dimensionless mol fraction of O_2 ($y_{O_2(g)}^{C}/y_{O_2(g),init}^{C}$) and is a function of both time and spatial dimension. ξ is the dimensionless spatial parameter (x^C/ℓ^C) and τ^C the dimensionless time defined as:

$$\tau^C = \frac{D_{O_2,eff}^{C}}{\varepsilon_{pore}^{C}(\ell^C)^2}\cdot t \quad (56)$$

Where $D_{O_2,eff}^{C}$ is the effective mass diffusivity of oxygen in the cell porous cathode and ε_{pore}^{C} is the pore volume fraction within the cathode. The parameter λ^C in Equation 55 is a dimensionless quantity indicative of the electrochemical reaction rate and is represented as:

$$\lambda^C = \frac{2k^C S^C_{eff} \rho^C_{bulk} (\ell^C)^2}{D^C_{O_2,eff}} \sinh\left(\frac{F\bar{\eta}^C_s}{RT}\right) \quad (57)$$

Here k^C is the intrinsic reaction rate coefficient at the temperature of interest, S^C_{eff} is the effective interfacial area between the reactive gaseous mixture and the porous cathode ρ^C_{bulk} is the bulk density of the composite solid in the cell cathode, and $\bar{\eta}^C_s$ is the electrochemical reaction surface overpotential averaged over the thickness of the cathode. The parameter γ^C in Equation 55 is a dimensionless quantity related to the operating current and is defined as:

$$\gamma^C = \frac{10F D^C_{O_2,eff} n^A_{H_2(g),init}}{I\varepsilon^C_{pore}(\ell^C)^2\left(1 - y^C_{H_2O(v),init}\right)} \quad (58)$$

It is noted that for the consumption of oxygen to produce oxide ions, the magnitude of λ^C must be greater than the magnitude $|1/(\gamma^C - \tau^C)|$. As soon as these two quantities would become equal, the consumption of oxygen would stop. Consequently, the production of oxide ions would end, resulting in the termination of the cell electric power delivery to any external circuit. The suitable set of the initial condition (IC) and boundary conditions (BC1 and BC2) to solve the PDE (Eq. 55), are given as follows:

$$IC: \quad \psi(\tau^C = 0) = 1 \quad for\ all\ \xi \in [0,1] \quad (59)$$

$$\text{BC1: } \psi(\xi{=}0) = \frac{1}{y^C_{O_2(g),init}}\left(\frac{y^C_{O_2(g),init}\gamma^C - \tau^C}{\gamma^C - \tau^C}\right) \text{ for all } \tau^C \in [0,\gamma^C) \quad (60)$$

$$BC2: \quad \left.\frac{d\psi}{d\xi}\right|_{\xi=1} = 0 \quad for\ all\ \tau^C \in [0,\gamma^C) \quad (61)$$

Here BC1 (Eq. 60) is a dimensionless form of Eq. 32. This PDE has been solved analytically for the following two cases:

Case I

The porous cell cathode is sufficiently thin (e.g. $\ell^C < 25\ \mu m$) and the operational conditions are such that spatial variation due to diffusion within the cathode can be neglected. Consequently, the PDE reduces to:

$$\frac{d\psi}{d\tau^C} = -\left(\lambda^C - \frac{1}{\gamma^C - \tau^C}\right)\psi \quad (62)$$

Which has solution (for values of $\tau^C < \gamma^C$):

$$\psi(\tau^C) = \frac{\gamma^C e^{-\lambda^C \tau^C}}{\gamma^C - \tau^C} \quad (63)$$

Case II

The porous cell cathode is thick enough (e.g. $\ell^C = 1\ mm$) that spatial variations due to diffusion within the cathode must be considered. Here the full PDE was solved analytically to yield $\psi(\tau^C, \xi)$ as a function of both time and depth in the porous cathode.

3. RESULTS AND DISCUSSION

Due to the complexity of the analytic solution for both derived PDEs[3] (Eqs. 46 and 55), these results were verified using standard numerical approaches. The two solution techniques provided indistinguishable results, with the differences between them $< 0.1\%$ for any given value of input parameters. Figures 2 and 3 in this section present both the numeric (points) and analytic solution (lines). Figures 2a through 2d show the transient ϕ vs ζ profiles within the SOFC porous anode for 4 different (α^A, λ^A) pairs. For each parametric set, ϕ decreases as the depth within the anode, ζ, increases for each value of dimensionless time, $\tau^A > 0$ until it flattens out due to the no-flux condition imposed by BC2 (Eq. 51). Also apparent, for any fixed value of ζ, the dimensionless mol fraction, ϕ decreases as time progresses and the fuel continues to be consumed via the electrochemical reaction. This decrease is more pronounced at higher values of λ^A which is indicative of a faster reaction rate.

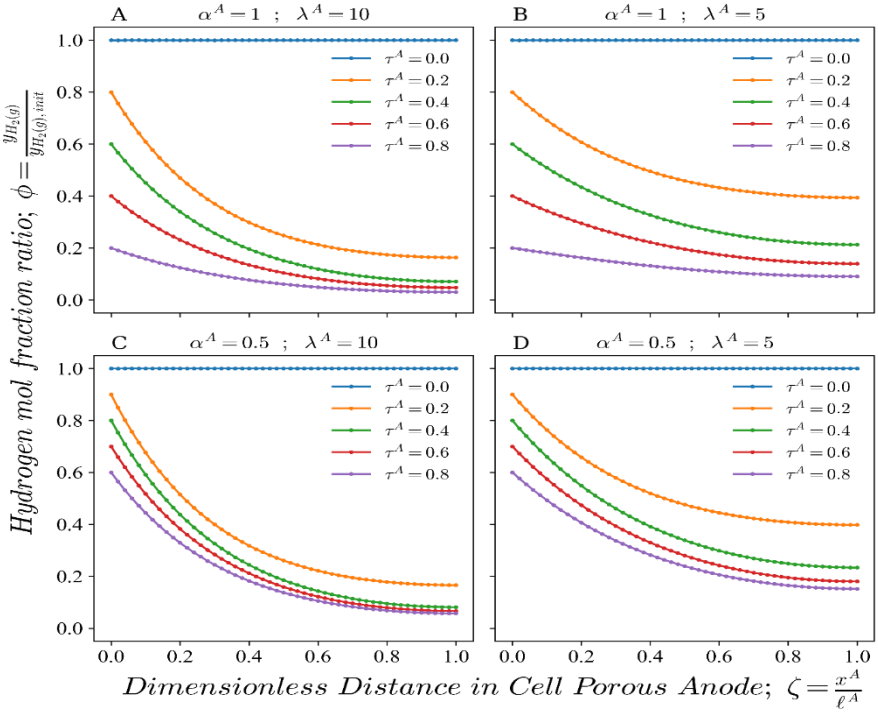

Figure 2. The transient profiles of $\phi = \frac{y_{H_2(g)}}{y_{H_2(g),init}}$ vs. the dimensionless distance $\zeta = \frac{x^A}{\ell^A}$ for various values of the parameters α^A and λ^A.

Figures 3a through 3d show the transient ψ vs ξ profiles within the SOFC porous cathode for 4 different (γ^C, λ^C) pairs using $y^C_{O_2(g),init} = 0.1$. For each parametric set, ψ decreases as the depth within the cathode, ξ, increases for each value of dimensionless time, $\tau^C > 0$ until it flattens out due to the no-flux condition imposed by BC2 (Eq. 61). Also apparent, for any fixed value of ξ, the dimensionless mol fraction, ψ decreases as time progresses and the oxidant continues to be consumed via the electrochemical reaction. This decrease is more pronounced at higher values of λ^C which is indicative of a faster reaction rate.

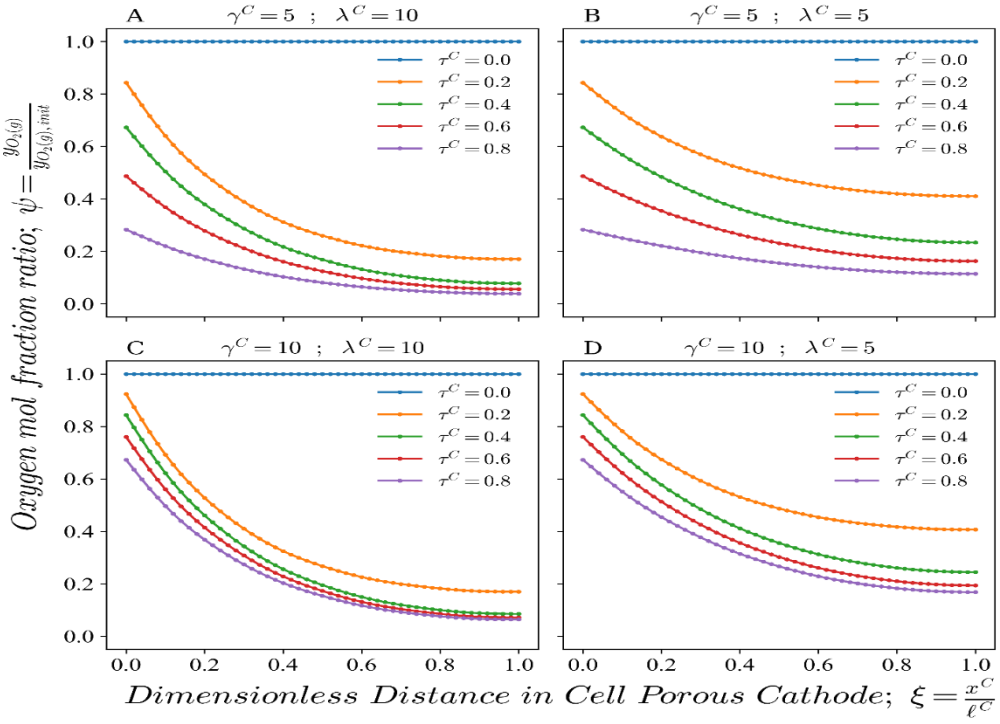

Figure 3. The transient profiles of $\psi = \frac{y_{O_2(g)}}{y_{O_2(g),init}}$ vs. the dimensionless distance $\xi = \frac{x^C}{\ell^C}$ for various values of the parameters γ^C and λ^C.

4. CONCLUDING REMARKS

The formulation presented in this relatively short paper was developed with the objective of its application to investigate the transient (i.e. non-steady state) behavior of a high temperature-solid oxide fuel cells such as that shown in Figure 1. At a fixed cell current level, the chemical species mole balances were applied over the cell anode-side fuel (hydrogen) and cathode-side oxidant (air) chambers to specifically predict the amount and composition of hydrogen and water vapor in the cell anode-side fuel chamber, and oxygen, nitrogen, and water vapor in the cell cathode-side oxidant chamber at any time during the cell operational period. The presented formulation also predicts the total pressures in the fuel and oxidant chambers.

Fundamentals of chemical and electrochemical engineering sciences were employed to develop the formulation to predict the transient mole fraction profiles of fuel (hydrogen) and oxidant (oxygen in air) in the SOFC porous anode and cathode, respectively, during the cell operational period. Numeric and analytical techniques were employed to solve the PDEs (Eqs. 46 and 55), to predict the transient mole fraction profiles of the fuel and oxidant within the anode and cathode respectively. This model captures both the effective diffusion rate of the fuel/ oxidant species within the anode/ cathode in response to the transient boundary conditions and their consumption via the electrochemical reaction with λ^A and λ^C as dimensionless kinetic parameters. The confidence in our computed values is improved due to the good agreement between the two different solution techniques.

With the use of very thin SOFC porous electrodes so that the second partial derivatives $\frac{\partial^2\phi}{\partial\zeta^2}$ and $\frac{\partial^2\psi}{\partial\xi^2}$ are negligible relative to the other terms in the PDEs (Eqs. 46 and 55), one can determine values for the dimensionless parameters λ^A and λ^C from Eqs. 54 and 63 via the collection of data on ϕ vs. τ^A and ψ vs. τ^C.

Finally, it is stated here that although in the formulation presented in this paper hydrogen and oxygen were used as the reactants of the high temperature SOFC of the type shown in Figure 1, the formulation scheme can be adapted for any material-type high temperature SOFC as well as for any fuel and oxidant composition combinations.

REFERENCES

1. S.S. Sandhu, K.R. Hinkle. Model for Prediction of Performance Behavior of a Solid Oxide Electrolyte Fuel Cell. (Submitted: Electrochemica Acta)
2. P. Han et al. Novel oxide fuel cells operating at 600-800ºC; An EPRI/GRI Fuel Cell Workshop on Fuel Cell Te4chnology Research and Development, New Orleans, LA. (1993).
3. K.R. Hinkle and S.S. Sandhu. Using Python and SymPy to Develop Analytical Solutions for Elliptic PDEs with Transient Boundary Conditions (Submitted: Chemical Engineering Education)